Available online at www.sciencedirect.com
ScienceDirect
Journal of Catalysis 243 (2006) 171–182
JOURNAL OF CATALYSIS
www.elsevier.com/locate/jcat

DRIFTS study of the water–gas shift reaction over Au/Fe_2O_3

B. Aeijelts Averink Silberova, G. Mul, M. Makkee *, J.A. Moulijn

DelftChemTech, Catalysis Engineering, Faculty of Applied Sciences, Delft University of Technology, Julianalaan 136, NL 2628 BL Delft, The Netherlands

Received 28 February 2006; revised 30 June 2006; accepted 6 July 2006

Available online 28 August 2006

Abstract

The water–gas shift (WGS) reaction over Au/Fe_2O_3 was studied by *operando* diffuse-reflectance infrared Fourier transform spectroscopy (DRIFTS) combined with mass spectrometry (MS). Au/Fe_2O_3 and Fe_2O_3 were exposed to high temperature (400 °C) in He, followed by CO, H_2, or H_2O treatment at 25 and/or 200 °C, respectively. The results showed that carbonate-like species and hydroxyl groups are present on the as-received sample, and not all of them are removed during high-temperature treatment at 400 °C. Although the dynamics of adsorbates on the catalyst surface have been observed at room temperature, at elevated temperature (200 °C)—that is, real operational steady-state conditions—the reduction–oxidation mechanism is the main pathway to the production of CO_2 and H_2. Formates have not been observed under these reaction conditions. At elevated temperature, the support Fe_2O_3, in the presence of Au particles is easily reduced and contributes the catalyst performance for the WGS reaction. The water introduced to Fe_2O_3 does not contribute to reoxidation to a large extent and, consequently, to high CO_2 production as observed over Au/Fe_2O_3. Furthermore, H_2 is evolved only in the presence of Au particles and when a certain degree of Fe oxide reduction is achieved.

Keywords: Water–gas shift reaction; Au; Mechanism; DRIFTS; TPR

1. Introduction

The pioneering work of Haruta et al. has initiated extensive research efforts on the application of nanosize gold in heterogeneous catalysis [1–5]. Haruta et al. have shown that gold on titania has extraordinary selectivity in epoxidation of propene, using a combination of hydrogen and oxygen as oxidant, as well as very high activity in low-temperature CO oxidation, which has been confirmed by others [3–10]. Various groups have analyzed the mechanism of Au-induced reactions [11–20], including the water–gas shift (WGS) reaction [20–39]. Various metal oxides have been reported to be active supports for Au particles in the latter reaction, including CeO_2 [20–29], TiO_2 [30–32], ZrO_2 [25,33], ZnO [25,33], Fe_2O_3 [25,28,31,33–37], Fe_2O_3-ZnO [25,33], Fe_2O_3-ZrO_2 [25,33], and zeolites [38], have all been discussed.

The reaction pathways of WGS reaction over gold-based catalysts have been addressed in some of these contributions [23,25,31,32,34]. Two reaction mechanisms generally can be considered for the WGS reaction: (i) the regenerative mechanism, which includes reduction of support sites by CO, yielding CO_2, followed by dissociation of H_2O to adsorbed O and H atoms (presumably on Au) and reoxidation of the reduced support sites with concomitant H_2 formation, and (ii) adsorptive mechanism comprising adsorption of CO and H_2O; formation of formate, carbonate, or bicarbonate intermediates (CO_yH_x); and finally decomposition of the intermediates to form CO_2 and H_2 [40]. The mechanisms are summarized as follows:

(i) regenerative

$$H_2O(g) \rightarrow H_2O(s),$$

$$H_2O(s) \rightarrow OH(s) + H(s),$$

$$OH(s) \rightarrow O(s) + H(s),$$

$$2H(s) \rightarrow H_2(g),$$

$$CO(g) \rightarrow CO(s),$$

* Corresponding author.
E-mail addresses: b.aeijeltsaverink-silberova@tudelft.nl (B. Aeijelts Averink Silberova), g.mul@tudelft.nl (G. Mul), m.makkee@tudelft.nl (M. Makkee), j.a.moulijn@tudelft.nl (J.A. Moulijn).

0021-9517/$ – see front matter
doi:10.1016/j.jcat.2006.07.010

$$CO(s) + O(s) \rightarrow CO_2(s),$$

$$CO_2(s) \rightarrow CO_2(g),$$

(ii) adsorptive

$$H_2O(g) \rightarrow H_2O(s),$$

$$CO(g) \rightarrow CO(s),$$

$$H_2O(s) + CO(s) \rightarrow CO_yH_x,$$

$$CO_yH_x \rightarrow CO_2(s) + H_2(s),$$

$$CO_2(s) \rightarrow CO_2(g),$$

$$H_2(s) \rightarrow H_2(g).$$

Besides the adsorptive mechanism through (bi)carbonates, in cases of the WGS reaction over Au/CeO_2 catalysts, Tabakova et al. have proposed an adsorptive mechanism with the involvement of formate species [23]. Jacobs et al. confirmed that formate species can be formed on the surface of reduced CeO_2 during the WGS [27]. These studies on ceria-based catalysts found that in steady-state WGS conditions, the ceria surface is present in a reduced state, as evidenced by in situ measurements [23]. In contrast, Jacobs et al. have excluded a ceria redox mechanism based on the observation that adding H_2O has resulted only in the formation of bridging OH groups by reaction with ceria vacancies [25].

Considering the WGS reaction over Au/Fe_2O_3 and Au/TiO_2, both the associated and regenerative mechanisms have been proposed to occur simultaneously [31,32,34,35]. The associative mechanism consisted of the dissociative adsorption of H_2O on small gold particles followed by spillover of activated hydroxyl groups onto adjacent sites of the ferric oxide [31,35]. This is followed by reaction of CO at the Au–support interface [34], eventually yielding CO_2 and H_2. Enhanced catalytic activity of Au/Fe_2O_3 compared with Fe_2O_3 was explained on the basis that Au/Fe_2O_3 contains more active OH groups [34]. In the event that the support is reduced by CO, H_2O molecules were reported to participate in the reoxidation Fe^{2+} to Fe^{3+} [34]. It should be noted that the IR spectra recorded by Boccuzzi et al. were obtained without measuring reaction products; that is, a direct connection between reaction products and the structure of the catalyst could not be made.

The present mechanistic study is focused on the WGS reaction over a reference Au/Fe_2O_3 catalyst of the World Gold Council (WGC) [3]. *Operando* diffuse-reflectance infrared Fourier transformation spectroscopy (DRIFTS) with mass spectrometry (MS) analysis of the gas composition has been applied to monitor the exposure of Au/Fe_2O_3 and Fe_2O_3 to CO, H_2O, and H_2 at 25 and/or 200 °C to correlate reaction products directly to compositional changes on the catalytic surface. The reducibility of the catalyst as measured by TPR is also discussed. The studies provide new insight into the initial morphological changes of the catalyst and reaction pathways at elevated temperature.

2. Experimental

2.1. Catalyst preparation and characterization

The applied Au/Fe_2O_3 reference catalyst was obtained from the WGC [3]. This catalyst was prepared by co-precipitation as described previously [47]. A final Au loading of 4.48% was determined by ICP analysis. Au particle sizes ranging from 3 to 5 nm [16,30] and a mean gold particle size of 2.8 nm [47] have been reported. The BET area of the calcined sample at 400 °C was 38.7 m^2/g [47].

Temperature-programmed reduction (TPR) of Au/Fe_2O_3 and Fe_2O_3 was performed with 7% H_2 in Ar and a total flow rate of 37 ml/min to further characterize the reducibility of the sample. The sample (100 mg) was diluted by SiC at a ratio of 1:1.5. A heating rate of 10 °C/min was chosen to reach 900 °C. The H_2 signal was recorded using TCD analysis.

2.2. DRIFT spectroscopy and mass spectrometry

DRIFTS studies were performed on a Thermo Nicolet Nexus IR with OMNIC software. The sample (∼50 mg) was first treated in a flow of (∼35 ml/min) He at 400 °C for 30 min (high-temperature treatment [HTT]) before each experiment. The heating rate during the treatment was 10 °C/min. After HTT, the sample was cooled under He to an operation temperature of either 25 or 200 °C. Unless stated otherwise, infrared (IR) spectra were recorded against a background of the sample at the reaction temperature under flowing He. IR spectra were recorded with co-addition 64 scans in single-beam spectra or absorbance spectra, by applying a resolution of 4 cm^{-1}. A Pfeiffer Vacuum ThermoStar mass spectrometer allowed direct identification of mass fragments of the reactants and products after interaction with the catalyst sample in the IR cell.

The catalyst (∼50 mg) was further exposed to CO, H_2O, H_2, or a mixture of CO (CTS, 2.0) and H_2O in He. The total flow rate was 32.2 ml/min. The CO (20% CO in Ar) was diluted by He to obtain a content of 0.5%. When H_2O was added, the H_2O content was 2.70%, obtained by saturating He in distilled H_2O at 25 °C and mixing with the CO/Ar stream.

The mixing device connected to the IR cell was equipped with a four-way valve allowing switching between a bypass line for an inert gas and a main line for the reaction mixture. In some experiments, the sample was heated under He flow at the end of the experiment to evaluate the released adsorbed species.

3. Results

3.1. High-temperature treatment

The products that evolved and the compositional changes that occurred from HTT of the Au/Fe_2O_3 catalyst as-received are shown in Fig. 1A (MS analysis) and Fig. 1B (IR spectra). A large amount of H_2O was released during HTT. The highest rate of formation occurred around 100 °C, followed by a smaller maximum at 220–225 °C. Furthermore, a signal of mass

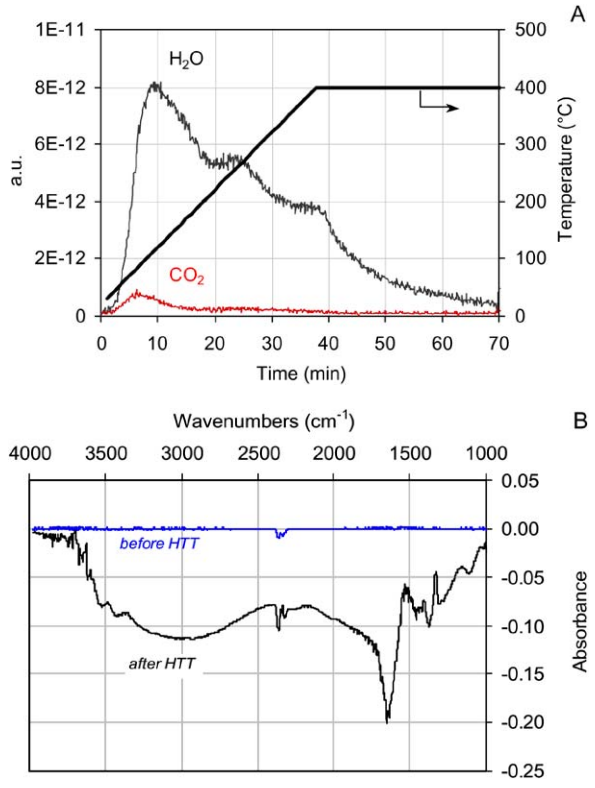

Fig. 1. HTT of the Au/Fe_2O_3 at 400 °C. Heating rate 10 °C/min in He flow. (A) Mass spectrometer analysis of H_2O and CO_2. (B) DRIFTS spectra before and after HTT; the spectra recorded against the background of the sample.

44 corresponding to CO_2 increased up to 75 °C. A small amount of CO_2 was then continuously released up to 400 °C.

FTIR spectra of the Au/Fe_2O_3 recorded at 25 °C in flowing He before and after HTT are shown in Fig. 1B. The spectrum recorded before HTT was recorded against the background of the sample, resulting in a straight line. In the spectrum recorded after HTT, the negative absorption bands were dominated by features centered at 3300 and 1650 cm^{-1}, assigned to the removal of adsorbed H_2O (in agreement with Fig. 1A). Additional changes can be seen in the spectral region of OH groups interacting with adsorbed H_2O at 3600, 3450, and 3380–2400 cm^{-1}. In addition, changes in the carbonate region (1000–1800 cm^{-1}) are prominent after HTT.

To further illustrate changes in the carbonate region, the DRIFTS spectrum of the HTT Au/Fe_2O_3 sample is compared with the spectrum of the sample as-received (Fig. 2), both recorded against a KBr background. On HTT, predominantly features of carbonate species were intensified, as evidenced by the increasing intensity at 1540, 1420, and 1330 cm^{-1}. This is most likely the result of the interconversion of bicarbonates into monodentate carbonate species, contributing to the evolution of H_2O at relatively high temperatures.

3.2. Temperature-programmed reduction

TPR profiles of the as-received Au/Fe_2O_3, HTT Au/Fe_2O_3, and HTT Fe_2O_3 are shown in Fig. 3. The support was reduced in several stages. The two-stage peak maximized at around

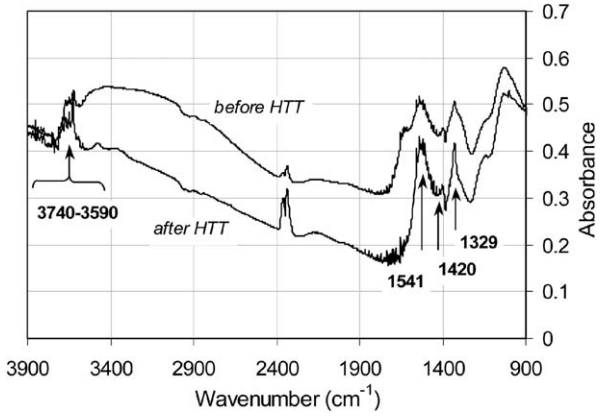

Fig. 2. DRIFT spectra of Au/Fe_2O_3 before and after HTT recorded against KBr spectra in a flow of He (25 ml/min) at 25 °C.

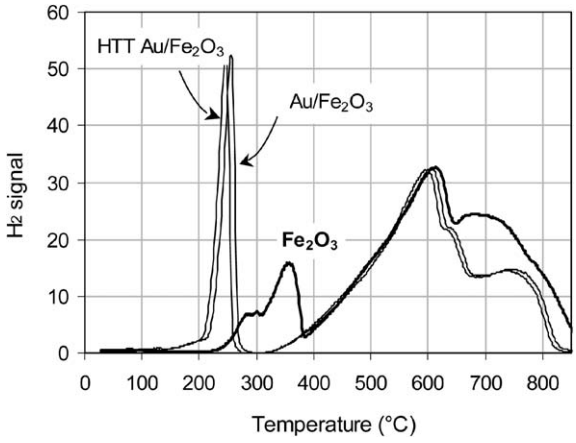

Fig. 3. TPR of Au/Fe_2O_3 as-received, HTT Au/Fe_2O_3 and Fe_2O_3 in a flowing H_2 (7% H_2 in Ar) and a heating rate of 10 °C/min.

360 °C is assigned to the reduction of Fe_2O_3 to Fe_3O_4 according to literature data [35,44,46]. The calculated ratio between the amounts of H_2 consumed below and above 400 °C amounted to 1/8, corresponding to the following reduction steps of Fe_2O_3:

$$Fe_2O_3 + \frac{1}{3}H_2 = \frac{2}{3}Fe_3O_4 + \frac{1}{3}H_2O,$$

$$\frac{2}{3}Fe_3O_4 + \frac{8}{3}H_2 = 2Fe + \frac{8}{3}H_2O.$$

A large, broad increase of the H_2 signal with a maximum at 620 °C obviously comprises several peaks that represent the multiple reduction steps of Fe_3O_4 to FeO and Fe [35,44,46]. TPR of Au/Fe_2O_3 revealed that Au lowered the reduction temperature of Fe_2O_3 to Fe_3O_4. In the presence of Au, this occurred as one large peak at around 250 °C. The change in carbonate species (Fig. 2) did not significantly influence the reduction temperature of Au/Fe_2O_3. The peak representing the reduction of Fe_2O_3 to Fe_3O_4 shifted only 10 °C lower. The observed effect of Au and HTT on the reduction of Fe_2O_3 has been previously reported [46] and is discussed further later in this paper.

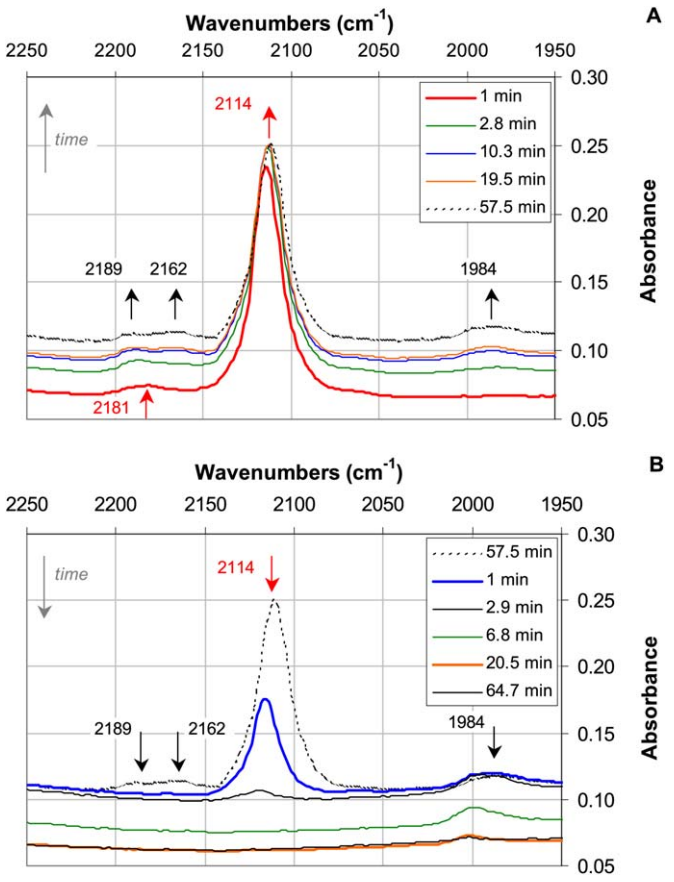

Fig. 4. Carbonyl region of DRIFTS spectra recorded during the exposure of HTT Au/Fe_2O_3 to CO/Ar/He at 25 °C (A) and after CO/Ar/He was switched off (B).

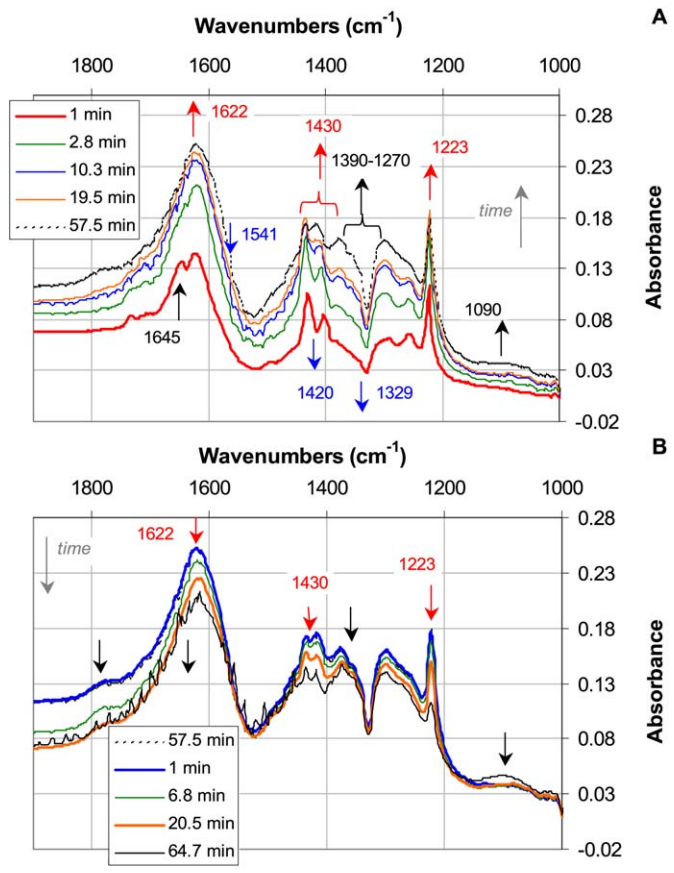

Fig. 5. Carbonate region of DRIFTS spectra recorded during the exposure of HTT Au/Fe_2O_3 to CO/Ar/He at 25 °C (A) and after CO/Ar/He was switched off (B).

3.3. *Au/Fe_2O_3 exposed to CO at 25 °C*

To study the interaction of CO with the Au/Fe_2O_3 catalyst, the catalyst was exposed to CO in the absence of H_2O at 25 °C after HTT treatment. Spectra recorded during 60 min on stream are shown in Figs. 4 and 5. The spectra are recorded against the background of the sample obtained just before the experiment. The carbonyl region is presented in Fig. 4. A large peak at 2114 cm^{-1} appeared in the first minute of the experiment and is generally assigned to CO linearly adsorbed on Au metallic sites [12,50]. This is in agreement with the fact that the catalyst after HTT contained mainly Au in a metallic state [31]. The band at 2114 cm^{-1} did not increase after 3 min on stream, indicating that at this stage all Au sites were covered with linearly adsorbed CO. The spectra recorded after the exposure to CO also revealed a band at 2189 cm^{-1}, which is characteristic for CO adsorbed on Fe^{x+} sites of the support [31,48]. The band at 2162 cm^{-1} was also observed after exposure of Au/FeO(111) to CO and assigned to weakly bound CO on small gold clusters that can undergo charge transfer due to a specific interaction with the support [50]. Adsorbed CO on the support sites was only weakly bound; these bands disappeared immediately after CO flow was switched off (Fig. 4B).

Fig. 4A also shows that when the catalyst was exposed to CO for longer time, a new broad band at 1984 cm^{-1} was formed. Metal carbonyl complexes are commonly found in the lower part of the region (2300–1900 cm^{-1}) [49]. Boccuzzi et al. [31] proposed that the band at 1990 cm^{-1}, which increased with CO coverage on reduced Au/Fe_2O_3, corresponds to bridge-bonded CO [31].

Desorption of CO induced by changing the gas composition to He results in a rapid decrease of the 2189 and 2162 cm^{-1} bands. The band at 2114 cm^{-1} decreases more slowly and takes at least 6.8 min to completely disappear.

On exposure of the HTT catalyst to CO at 25 °C, significant changes in the carbonate region of the spectrum also can be observed. The bands assigned to bidentate carbonate-like species (at 1540, 1420, and 1330 cm^{-1}) present on Au/Fe_2O_3 after HTT (Fig. 2) decreased during exposure to CO (Fig. 5A). The bands at 1622, 1430, and 1223 cm^{-1} (Fig. 5A), which are influenced by the negative spectral contributions of the bidentate species (especially of the band at 1430 cm^{-1}), increased immediately. These bands are characteristic of the stretching vibrations of bicarbonate species [13,31].

The bands located at 1645, 1390–1270, and 1070 cm^{-1} (Fig. 5A) also increased during exposure to CO. These bands can be assigned to other types of carbonate-like species [23,31]. Note that a peak at 1645 cm^{-1} did not increase over time as much as the band of bicarbonates did (at 1622 cm^{-1}). The peak with a maximum at 1622 cm^{-1} of an asymmetric shape

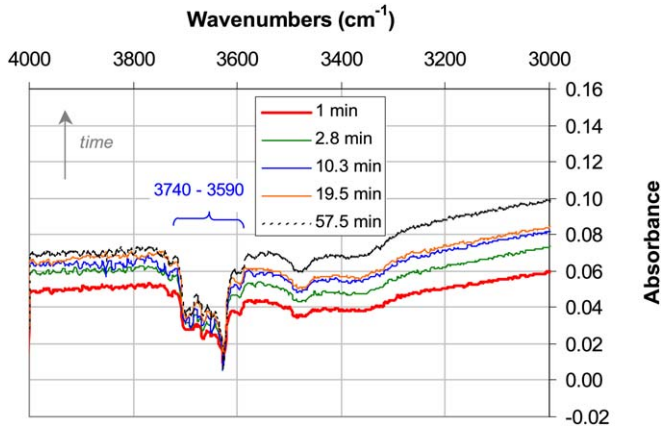

Fig. 6. DRIFTS spectra recorded during the exposure of HTT Au/Fe_2O_3 to CO/Ar/He at 25 °C.

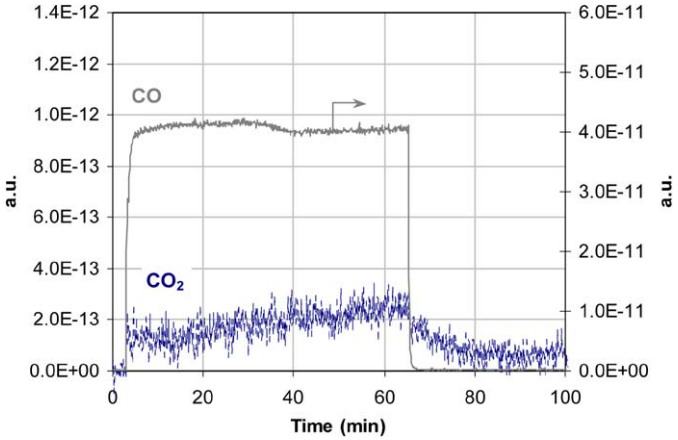

Fig. 7. Mass spectrometer analysis of Ar and CO_2 recorded during the exposure of HTT Au/Fe_2O_3 to CO/Ar/He at 25 °C and after CO/Ar/He was switched off.

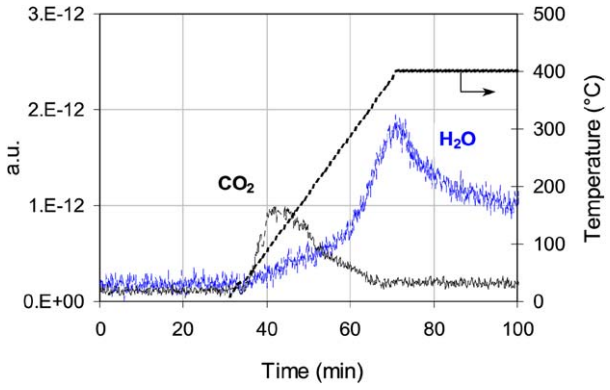

Fig. 8. Mass spectrometer analysis of H_2O and CO_2 when the sample exposed to CO/Ae/He at 25 °C was heated up to 400 °C (10 °C/min) in a flowing He.

comprised the band at 1645 cm^{-1} in the spectrum obtained at 77.2 min. This band indicates that carbonates species are easily formed on the surface and are strongly bonded. A broad band in the region at 1390–1270 cm^{-1} typical for the formation of carbonate-like species was again influenced by a decrease in the bidentate species (at 1330 cm^{-1}) present before the experiment.

After the CO flow was switched off (Fig. 5B), the bands of bicarbonates and carbonate-like species decreased with time. The bands typical for the bicarbonates disappeared faster than those for the carbonate-like species.

The results described above show that adsorbed CO was converted on the Au/Fe_2O_3 catalyst to carbonate/bicarbonate species. This observation agrees with changes in the hydroxyl group bands in the region 3590–3740 cm^{-1} (Fig. 6). Hydroxyl groups that were initially present on the support after HTT (Fig. 2) obviously participated in the transformation of linearly adsorbed CO on the metallic Au particles to yield carbonates and bicarbonates. Once the flow of CO was switched off, the negative minimum at ∼3700 cm^{-1} increased. This indicates that OH groups were reactive to form carbonate/bicarbonate species even when CO was not present in gas phase; that is, adsorbed and activated CO caused changes in the carbonate composition, rather than a direct interaction of OH groups with gas-phase CO.

The corresponding changes in gas-phase composition on introduction of CO to the HTT catalyst at 25 °C are shown in Fig. 7. A very small amount of CO_2 (mass 44) slightly and gradually increased during the CO exposure. This suggests that at room temperature, some conversion of CO to CO_2 occurred, albeit slowly, presumably through reaction and decomposition of the carbonate species observed in the IR spectra of Fig. 5. It is shown that some specific carbonate-like species remained on the surface even after the catalyst was maintained under a He flow for more than 1 h at 25 °C (Fig. 5B). Desorption of CO_2 and H_2O was induced by heating (at a rate of 10 °C/min) to 400 °C in He (Fig. 8). A maximum release of the CO_2 was observed at 88–113 °C. An increase in the H_2O signal up to 400 °C indicates that the catalyst—or, more specifically, the support—readsorbed some H_2O during the decomposition of (bi)carbonates at low-temperature experiments in CO.

3.4. *Au/Fe_2O_3 exposed to CO at 200 °C*

The reducibility of Au/Fe_2O_3 by CO was further investigated by DRIFTS, as shown in Fig. 9A. The spectra were recorded against the background of the sample before exposure to CO at 200 °C in a flow of He. When HTT Au/Fe_2O_3 was exposed to CO, the overall baseline of the spectra shifted to higher absorbance (Fig. 9A), indicating a change in the color affecting the reflection of the sample. Significant changes in the carbonate composition were not observed, although a slight increase is apparent in Fig. 9A.

3.5. *Au/Fe_2O_3 exposed to H_2 at 200 °C*

An overall shift of the baseline in the DRIFTS spectra was also observed when the catalyst was exposed to H_2 at 200 °C (Fig. 9B). Comparing the spectrum obtained immediately after exposure with the spectrum obtained at 34.3 min clearly indicates that sample reduction was a continuous process that did not end during the experiment. The shape of these spectra was similar to that of Au/Fe_2O_3 when exposed to CO (Fig. 9A). This indicates that the catalyst was indeed reduced when CO was present in the feed. Once the flow of H_2 was switched off

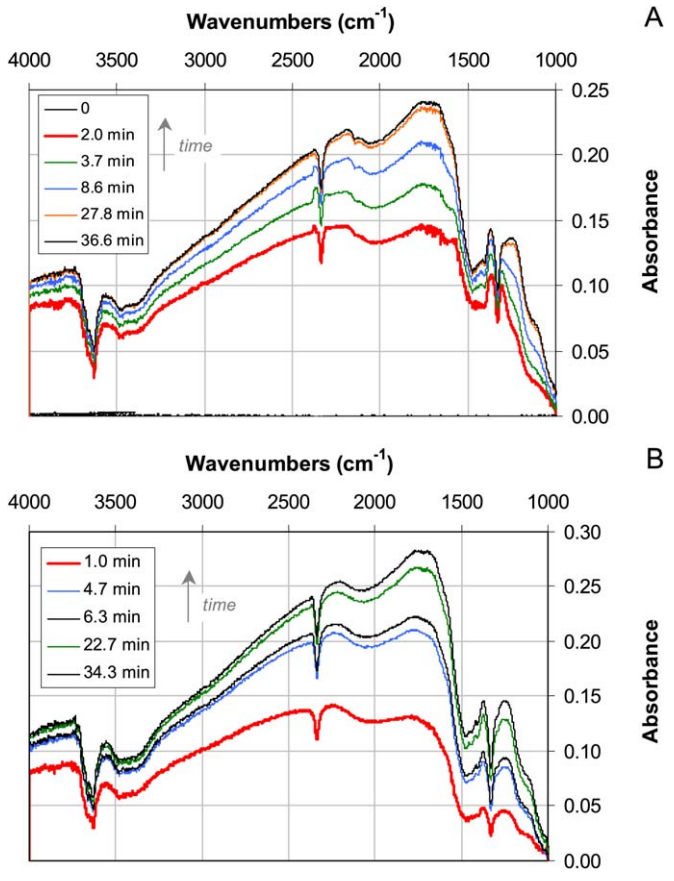

Fig. 9. DRIFTS spectra recorded during the exposure of HTT Au/Fe_2O_3 to CO/Ar/He (A) and H_2/He (B) at 200 °C.

and the catalyst was kept only under a flowing He, the catalyst reduction ended.

3.6. Au/Fe_2O_3 exposed to H_2O at 200 °C

The DRIFTS spectra recorded during the exposure of HTT Au/Fe_2O_3 to H_2O/He shown in Fig. 10A reveal an intense peak with a maximum at 1635 cm^{-1} in the region of the bending modes of adsorbed H_2O [5,31]. Two broad peaks of maxima at 3429 and 3217 cm^{-1} appear as a result of hydroxyl groups in dehydrated conditions interacting with adsorbed H_2O. Due to H_2O adsorption/reaction, interconversion of carbonates to bicarbonates was observed by DRIFTS, whereas decomposition to CO_2 and H_2 was not apparent (Fig. 12B). H_2O alone was unable to convert the carbonate species present to the final products.

3.7. Au/Fe_2O_3 exposed to CO and H_2O at 200 °C

The *operando* spectra of the catalyst during the WGS reaction at 200 °C are shown in Fig. 10B. It is obvious that the overall baseline shifted by ca. 0.25 absorbance units, indicating that the reflectance and thus the reduction state of the sample changed on reaction. This leads to the very important conclusion that the catalyst is, at least to a significant extent, in a reduced state in steady-state WGS reaction.

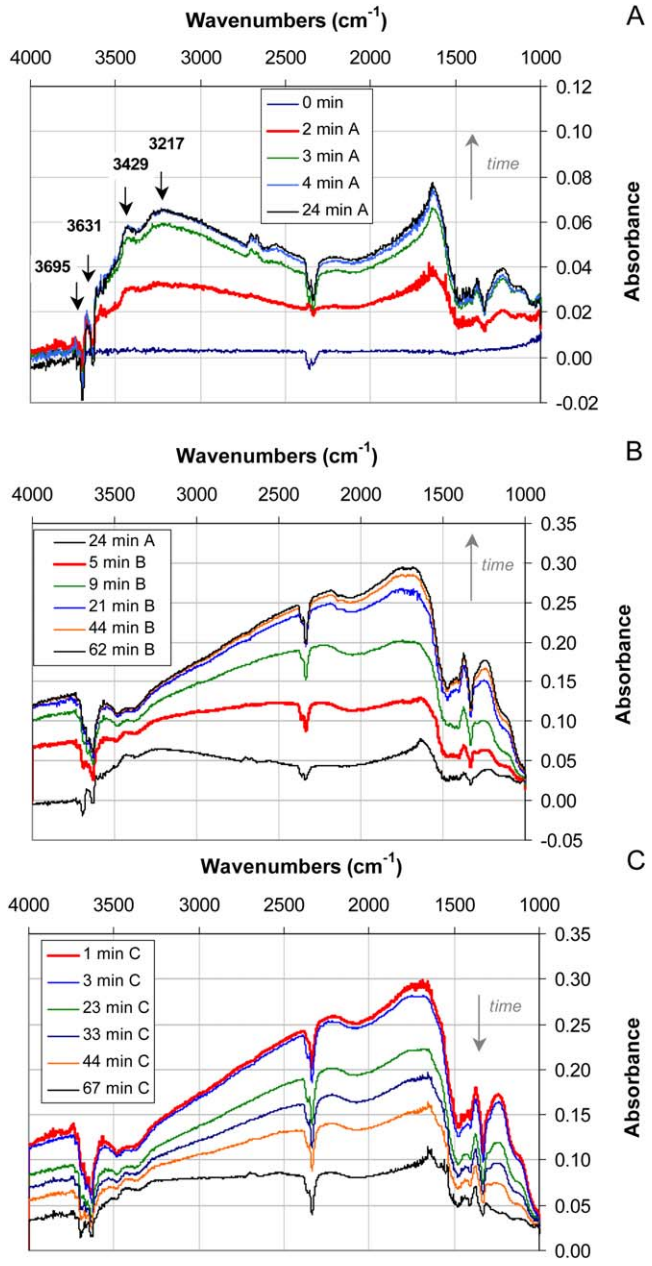

Fig. 10. DRIFTS spectra recorded during the exposure of HTT Au/Fe_2O_3 to H_2O/ He at 200 °C (A), followed by the exposure to CO/Ar/H_2O/He at 200 °C (B) and when CO/Ar/H_2O were switched off (C).

The spectra recorded when both CO and H_2O were switched off are presented in Fig. 10C. Reoxidation of the catalyst is indicated by the gradually changing baseline shift to that of the catalyst before reaction. Apparently the adsorbed H_2O and/or H_2O in the transfer lines could reoxidize the catalyst. We discuss this further in terms of the gas-phase products evolved during the transients in reactant composition.

3.8. Fe_2O_3 exposed to CO/H_2O mixture at 200 °C

Operando spectra of HTT Fe_2O_3 (i.e., without gold) are presented in Fig. 11. Intense negative peaks at 3682 and 3643 cm^{-1} indicate that OH groups of Fe_2O_3 were removed by HTT.

A baseline shift occurred after 5 min, although the change was less prominent than that seen for Au/Fe_2O_3.

In contrast with Au/Fe_2O_3, on exposure of Fe_2O_3 to CO/H_2O, an apparent increase of IR bands at 1560, 1440, 1270–1350 cm^{-1} (Fig. 11) occurred, and small features in the spectral range of C–H stretching frequencies also became visible. These spectral features have been assigned to the formation of formates [27]. Note that these bands appeared only after ca. 80 min of exposure to CO and H_2O.

3.9. Reactant/product evolution during exposure

Mass spectrometer analysis recorded during the exposure of Au/Fe_2O_3 catalyst to CO/Ar at 200 °C is presented in Fig. 12A. A maximum of CO_2 was observed within 1.8 min of the introduction of CO. After 10 min, the CO_2 response gradually decreased due to depletion of the oxygen available in the catalyst for CO_2 formation.

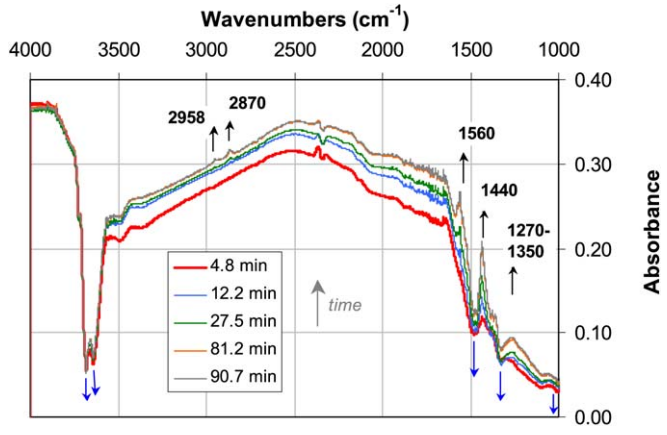

Fig. 11. DRIFTS spectra recorded during the exposure of HTT Fe_2O_3 to $CO/Ar/He/H_2O$ at 200 °C. The spectra were recorded against the single beam spectra of the sample before the exposure of the reaction mixture.

When HTT Au/Fe_2O_3 catalyst was exposed to the H_2O/He flow at 200 °C (Fig. 12B) (i.e., in the oxidized state), H_2 was not formed; the low H_2 response (around 1% of the H_2O signal) corresponded to fragmentation of H_2O in the mass spectrometer. Furthermore, no CO_2 was produced. Also note that the H_2O response increased irregularly with time, due to dynamics in feed concentration.

When the HTT Au/Fe_2O_3 catalyst was first exposed to the H_2/He flow at 200 °C (i.e., the catalyst partly in the reduced state) and later to the H_2O/He flow, H_2 was formed. The H_2 response initially increased, then decreased, and was significantly higher than observed as only a fragmentation of the H_2O. When HTT Fe_2O_3 was partly prereduced by H_2 at 200 °C and then exposed to the H_2O, no H_2 production was observed.

When HTT Au/Fe_2O_3 was exposed to a mixture of $CO/H_2O/Ar$ at 200 °C (Fig. 12C), important transients in the product composition were seen. The CO_2 production reached a maximum after 1.4 min with no release of H_2 by the catalyst system. H_2 was formed only after 2.2 min, once the CO_2 production rate reached a near-steady-state level. The response of H_2 then gradually increased, due in part to the increasing feed concentration of H_2O.

The product distribution obtained during the *operando* WGS reaction over Fe_2O_3 is presented in Fig. 12D. Although reduction of the catalyst (in agreement with the DRIFTS spectra) was accompanied by CO_2 release, the amount was at least 2.5 times lower than that produced over Au/Fe_2O_3. Furthermore, the response of CO_2 decreased rapidly with time, while H_2 was not formed over Fe_2O_3 in the applied conditions. Apparently, Au plays an essential role in the formation of H_2.

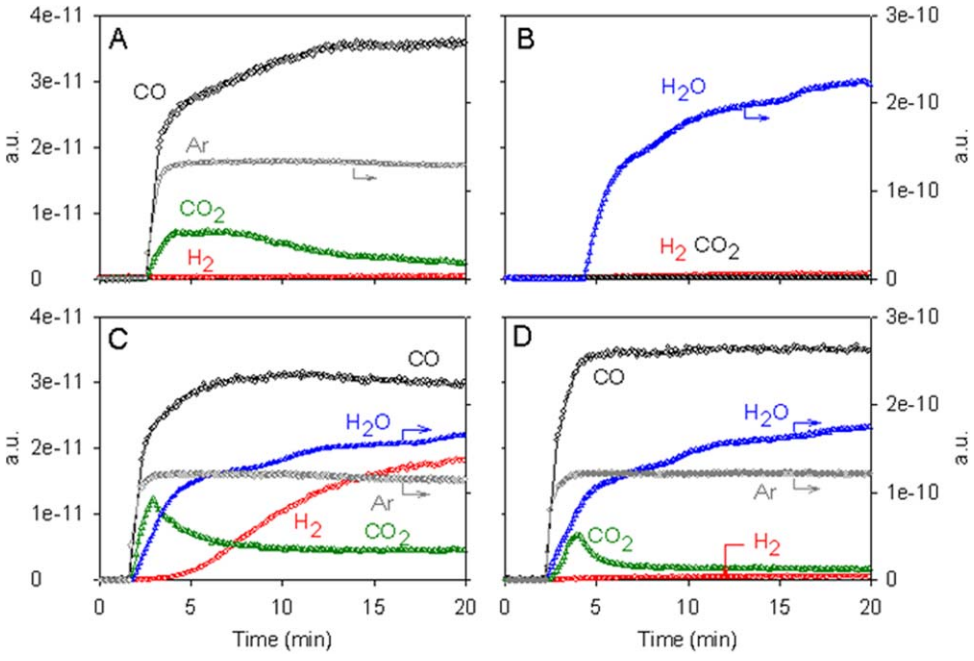

Fig. 12. Mass spectrometer analysis during the exposure of HTT Au/Fe_2O_3 to CO/Ar/He (A), H_2O/He (B), $CO/Ar/H_2O$/He (C) at 200 °C and the exposure of HTT Fe_2O_3 to $CO/Ar/H_2O$/He at 200 °C (D).

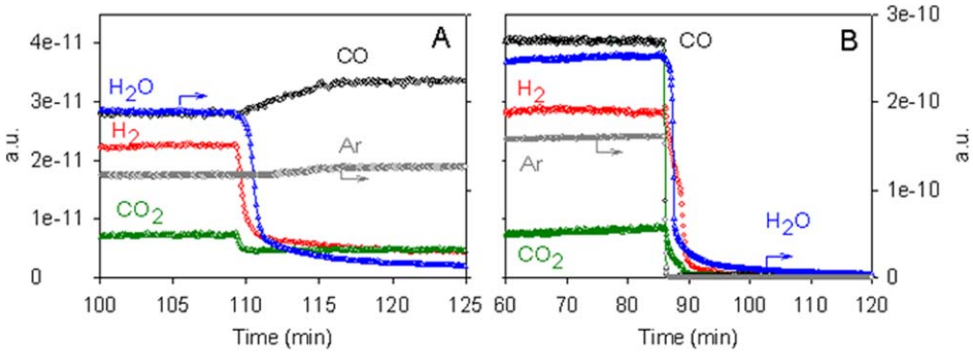

Fig. 13. Mass spectrometer analysis during the exposure of the HTT Au/Fe_2O_3 to CO/Ar/H_2O/He at 200 °C. (A) H_2O switched off. (B) CO/Ar/H_2O switched off.

To further assess the dynamics of the Au/Fe_2O_3 catalyst, various transient experiments were performed. In the first experiment, H_2O was discontinued after 106 min on stream (Fig. 13A), and the production of H_2 and CO_2 responded immediately. The rapid decrease in CO_2 production is again an indication that in steady-state conditions the catalyst is in a reduced state, leaving no oxygen to react with CO to CO_2, once H_2O is removed from the reactant mixture. Fig. 13B shows that when both CO and H_2O were switched off, CO_2 and H_2 production decreased within a couple of minutes. The discontinuities in the H_2 and CO_2 signals are ascribed to H_2O remaining in the system.

When CO was added to the mixture of H_2O/inert (see Fig. 12B), a transient appeared similar to that seen after the simultaneous introduction of CO and H_2O as reported in Fig. 12C. A maximum CO_2 production occurred, followed by initiation of H_2 production after 10 min. A gradual increase in H_2 response occurred for the next 25 min. After 60 min of the experiment, the CO, CO_2, H_2, and H_2O responses were stable.

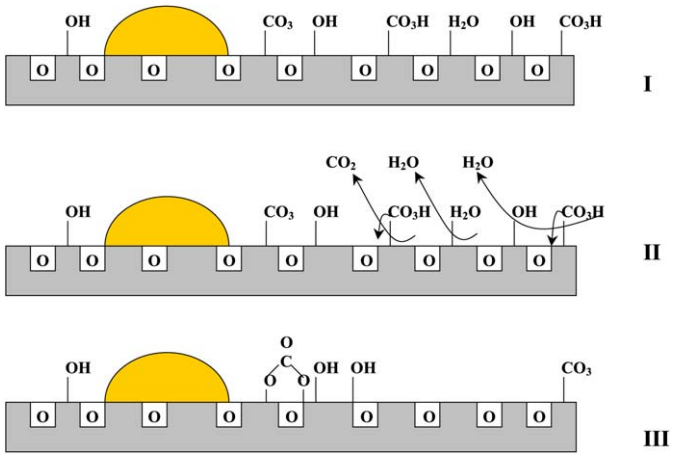

Fig. 14. Schematic model of HTT: I—Au/Fe_2O_3 (as-received) contains carbonate-like species and hydroxyl groups, II—HTT causes the desorption of CO_2 due to the decomposition of bicarbonates, the desorption of H_2O and the formation of carbonate-like species, III—after HTT, Au/Fe_2O_3 contains bidentate carbonate species, hydroxyl groups and new-formed carbonates.

4. Discussion

The preparation of gold-based catalyst is crucial to achieving high activity for reactions of CO [1,5,8,19,24,32,41–45]. This includes calcination conditions and heat treatment before initiation of the reaction [16,19,24,25,42–44,46]. Based on the information described in the literature, the oxidation state of the Au/Fe_2O_3 catalyst before exposure to experiments can be described as follows: The nanosize Au particles are predominantly in a metallic form [16,30,51], and supported on haematite (α-Fe_2O_3) [16,18]. In the present study, a combination of DRIFTS and MS analysis shows that additional HTT of the Au/Fe_2O_3 in flowing He up to 400 °C removes a significant amount of H_2O and OH-groups from the catalyst, whereas interconversion of bicarbonate to monodentate carbonate species is accompanied by slow decomposition to CO_2 (Fig. 2). The monodentate carbonate species are not entirely removed by HTT and are strongly bound to the support surface.

The DRIFTS results further indicate that linearly adsorbed CO, possibly bridge-bonded to a minor extent [31], is present on the Au metallic particles (Fig. 4A) at room temperature in the presence of CO. A small amount also adsorbs on Fe^{2+} sites generated by prolonged exposure to CO [31]. A decrease in the bands assigned to the bidentate carbonate remaining on the support after HTT occurs when HTT Au/Fe_2O_3 is exposed to CO at room temperature (Fig. 5A). This indicates that CO activated over the Au sites is reactive toward these carbonates and, moreover, that these carbonates are most likely present in the vicinity of the Au particles. Presumably, this reaction is responsible for the small amount of CO_2 produced. Furthermore, an increase in the bands typical for bicarbonates suggests that linearly adsorbed CO on metallic Au particles is also reactive toward hydroxyl groups on the support. Indeed, bicarbonate formation is accompanied by the consumption of OH groups (Fig. 6). These OH groups are not removed by HTT at 400 °C in a flowing He before the experiment, but are reactive once CO is adsorbed on the catalyst. Initially, hydroxylcarbonyls are formed; then the formation of bicarbonate species can proceed via the reaction of these hydroxylcarbonyls with available lattice oxygen at the Au–Fe_2O_3 interface. Most of the carbonate-like species remained on the catalyst at 25 °C (Fig. 5B). At elevated temperatures, these species decompose to CO_2 (Fig. 8). A schematic model of HTT is presented in Fig. 14.

Summarizing, DRIFTS spectra recorded at 25 °C show that CO is linearly adsorbed and activated on metallic Au particles (Fig. 4B) and can react with bidentate carbonate species on the

support surface, yielding CO_2, as well as with hydroxyl groups, resulting in bicarbonate formation and reduction of Fe^{3+} sites to Fe^{2+}. DRIFTS data recorded on HTT Au/Fe_2O_3 at 200 °C show no linearly adsorbed CO, whereas the bands assigned to bidentate carbonate and bicarbonate show similar trends as observed at room temperature (Fig. 9A). The main reaction occurring at 200 °C is reduction of the support, as indicated by dramatic changes in the baseline of the DRIFTS spectra, in agreement with the TPR data. Based on the TPR results, only the reduction of Fe_2O_3 to Fe_3O_4 appears likely, because reduction to Fe requires temperatures above 200 °C. Comparison of DRIFTS spectra recorded during the exposure of the catalysts to H_2 and CO (Figs. 9A and 9B) confirms that the changes in the baseline are related to reduction of the catalyst and not to some accumulation of deposits on the catalyst surface. The reduction of the catalyst by CO results in the production of CO_2 seen on MS in the initial stages of the reaction in both the absence and presence of H_2O (Figs. 12A and 12C). Note that reduction of the support is promoted by the presence of Au, as is evident from the TPR results and the much smaller baseline shift for Fe_2O_3 shown in Fig. 11. Oxygen will be available for CO_2 production at the interface between the Au particles and the support. CO consumption is rather low, because bulk diffusion of oxygen to the surface vacancies is slow and represents a limiting step in the reduction mechanism. The abstraction by CO of Fe_2O_3 lattice oxygen in Au/Fe_2O_3 was described elsewhere [13,42]. It was attributed to the presence of nanosize gold particles that promote this process due to their inherently defective structural sites [13,42]. It has also been suggested that the energy evolving during the chemisorption of CO is responsible for a surge in temperature at the Au–Fe_2O_3 interface that contributes to the accelerated reaction between CO and the support [13,42]. The exact mode of Au promoting the reduction of Fe_2O_3 is not known at this moment, and requires further investigation.

DRIFTS data reveal that H_2O adsorbs on the Au/Fe_2O_3 catalyst at 200 °C (Fig. 10A), strongly interacting with surface hydroxyl groups. Boccuzzi et al. [31] reported that H_2O and OH groups are located everywhere, including on the support, on gold sites, and at the interface between them. Evidence for H_2O–Au interactions was not obtained from the present study; only interaction with the support sites can be confirmed. Mass analysis showed that the exposure of the catalyst to H_2O is not accompanied by desorption of products (Fig. 12B). Nevertheless, H_2 production was observed during the exposure to H_2-prereduced catalyst to H_2O. This observation supports the regenerative mechanism for the WGS reaction on Au/Fe_2O_3 occurring in steady-state conditions (i.e., 200 °C). DRIFTS spectra recorded after exposure of a partly reduced (by CO/H_2O/inert flow) Au/Fe_2O_3 to a H_2O environment (Fig. 10C) show reoxidation of the surface. When the reflectance of the sample is taken as measure for the degree of catalyst reduction, the time needed for reoxidation of the catalyst is significantly longer than that needed for reduction by CO; the reoxidation step is thus rather slow and perhaps rate-limiting in the WGS reaction.

The *operando* DRIFTS spectra can be discussed as follows. Once HTT Au/Fe_2O_3 is exposed to CO and H_2O at 200 °C (Fig. 12C), in the initial stages carbonates are decomposed, while CO reduces the catalytic surface. The dissociation of H_2O leads to the formation of H_2. For HTT Au/Fe_2O_3, H_2 is formed with a certain time delay (Fig. 12C). H_2 production starts when the CO_2 signal decreases slightly. It is obvious that H_2 will participate in the initial reduction of the catalyst (Figs. 3, 9B, 12C). Once a certain reduction degree is obtained, H_2 will be formed and released.

The present experiments clearly show that H_2 is not formed on HTT Fe_2O_3 under exposure to CO and H_2O (Fig. 12D) but is formed only when Au particles are present. This indicates that the support itself is unable to allow this step to occur at a significant rate. The DRIFTS spectra also show that formate species are formed on the support in the absence of Au after 80 min of exposure to CO and H_2O (Fig. 11). Compared with the MS analysis corresponding to this experiment, the observed formates in this case are only spectators and do not participate in the formation of CO_2, which was observed only at the beginning of the experiment. At the time when formates are formed, almost no CO_2 is detected. Therefore, a release of CO_2 on Fe_2O_3 under these conditions results only from the reduction of Fe_2O_3 by CO.

The essential role of Au in H_2 production merits further discussion. Two modes of operation can be postulated. The first mode involves activation of H_2O directly on reduced Fe sites (possibly in the vicinity of the Au particles), followed by reverse spillover and release of H_2. The other mode is activation of H_2O primarily on the Au particles, followed by dissociation of H_2O and further reaction to H_2. The dissociative adsorption of H_2O on small gold particles followed by a spillover of activated hydroxyl groups onto adjacent sites of the ferric oxide was reported previously [31,34,35]. Unfortunately, however, which of these two modes is truly operating cannot be determined based on our experiments. Nevertheless, it is important to note that the presence of water in the WGS reaction performed over Fe_2O_3 does not lead to high production of hydrogen (Fig. 12D). The Au particles are crucial to hydrogen production under these conditions (Fig. 12C).

The evolution of CO_2 is higher at the increased temperature. The maximum rates of CO_2 production at 200 °C are more than 40 times faster than the rates at 25 °C (Table 1). At 200 °C, initial rates of CO_2 evolution on Au/Fe_2O_3 in 0.5 min after the exposure to CO and to CO and H_2O (Table 1) indicate that the presence of H_2O causes slightly faster evolution of CO_2. The rates decrease after reaching the maximum after 1.9 min of exposure. With exposure of the Au/Fe_2O_3 to CO, the rates decrease gradually over time. Nevertheless, when H_2O is present, the constant rates of CO_2 evolution (0.01 $\mu l/h/g_{cat}$) are reached after 5 min of exposure.

Table 1 gives the rates of the CO_2 evolution obtained via the exposure of Fe_2O_3 to CO and H_2O. The maximum rate at 1.9 min was not as high as that over Au/Fe_2O_3. The water in the WGS reaction acts as an oxygen source for the continuous production of CO_2. For Fe_2O_3, the rate of CO_2 production decreases even though water is present (Table 1).

Table 1
CO_2 evolution rate after the exposure to CO or to CO + H_2O during DRIFTS experiments

Time after the exposure (min)	CO Au/Fe_2O_3 25 °C		CO Au/Fe_2O_3 200 °C		CO + H_2O Au/Fe_2O_3 200 °C		CO + H_2O Fe_2O_3 200 °C
	(μl/h/g_{Au})	(μl/h/g_{cat})	(μl/h/g_{Au})	(μl/h/g_{cat})	(μl/h/g_{Au})	(μl/h/g_{cat})	(μl/h/g_{cat})
0.5	0.010	0.0004	0.18	0.008	0.27	0.01	0.006
1.9	0.007	0.0003	0.35	0.016	0.48	0.02	0.011
2.5	0.005	0.0002	0.33	0.015	0.41	0.02	0.007
5.0	0.005	0.0002	0.33	0.015	0.28	0.01	0.005
10.0	0.008	0.0004	0.20	0.009	0.23	0.01	0.004
15.0	0.003	0.0002	0.13	0.006	0.22	0.01	0.004
20.0	0.008	0.0004	0.11	0.005	0.23	0.01	0.003

The *operando* DRIFTS MS experiments present herein were run at the conditions close to the continuous-flow experiments performed in the six-flow setup [52]. The total flow rate for the *operando* WGS experiments (32.5 ml/min) is comparable with that used for the continuous-flow experiments (55 ml/min) in the six-flow setup [52]. The CO conversion of 34% obtained in our steady-state conditions is close to the conversion over Au/Fe_2O_3 at 200 °C in the continuous-flow experiment [52].

Based on the foregoing observations; the state of Au/Fe_2O_3 before the experiment, as well as the reaction pathways for the WGS reaction over HTT Au/Fe_2O_3 (WGC) at 200 °C can be summarized as follows:

- Linear adsorption of CO occurs predominantly on metallic Au particles. Adsorbed CO influences the decomposition of the carbonate-like species remaining on the Fe_2O_3 surface after HTT (Fig. 15, steps IV–VI).
- Linearly adsorbed CO reacts alternatively with OH groups to form hydroxylcarbonyl. Oxygen atoms at the Au–support interface participate in the formation of bicarbonates being decomposed to CO_2 in a next step (Fig. 15, steps IV–VII). Bicarbonate also reacts with OH groups, leading to H_2O release and carbonate species (Fig. 15, steps VII–X).
- Removal of oxygen atoms from Fe_2O_3 and the Au–Fe_2O_3 interface leads to reduction of the support, and CO_2 is produced. This step is accompanied by oxygen bulk diffusion appearing as a slow step (Fig. 16, steps XI–XIII).
- H_2O adsorbs dissociatively and is promoted in the presence of Au particles; hydroxyl groups are able to reoxidize the support (Fig. 16, steps XIV–XVI).
- H_2 participates in the reduction of the support (Fig. 17, step XVII). Linearly adsorbed CO reacts with OH groups to form hydroxylcarbonyl, which reacts in the next step with lattice oxygen to form bicarbonates and spillover to the Au–support interface (Fig. 17, steps XVIII–X). When a certain reduction state of Au/Fe_2O_3 is achieved, the hydrogen atoms react and H_2 is produced (Fig. 17, steps XXI–XXII). H_2 is formed not on Fe_2O_3, but rather at the Au–Fe_2O_3 interface.

A whole scenario points out that both the adsorptive and regenerative mechanisms occur for the WGS on Au/Fe_2O_3. The

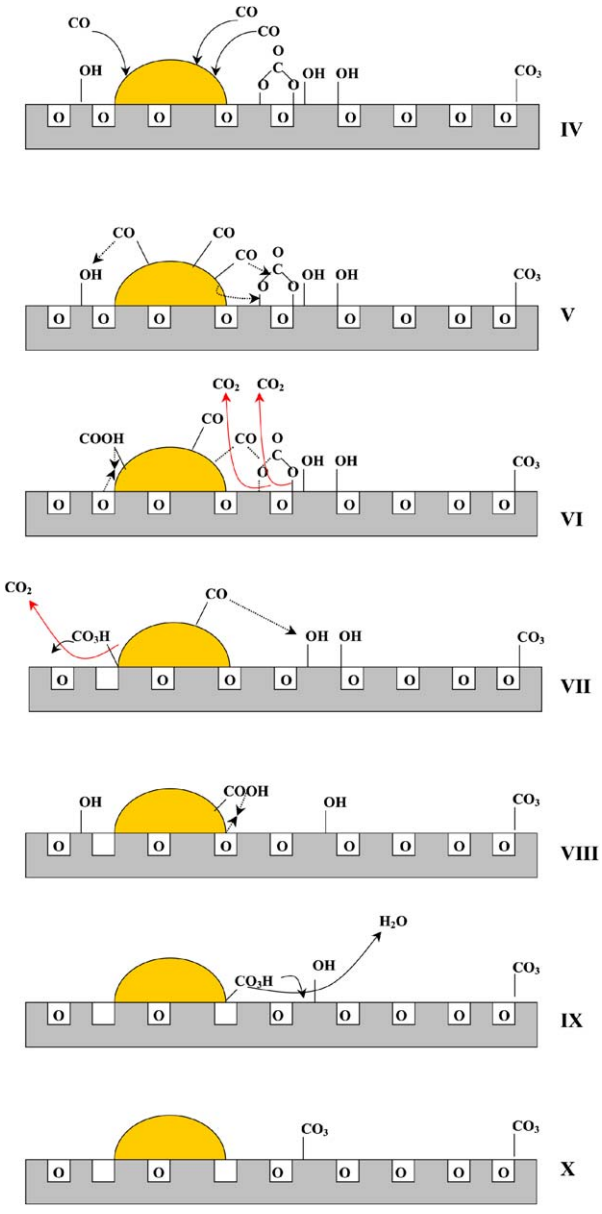

Fig. 15. Schematic model of WGS: IV—linear adsorption of CO on the metallic Au particles; V, VI—decomposition of present bicarbonate species, formation of hydroxylcarbonyl and spillover to Au–support interface; VII—formation of bicarbonates and their decomposition to CO_2 and OH; VII–X—formation and decomposition of bicarbonate species to carbonates accompanied by the H_2O desorption.

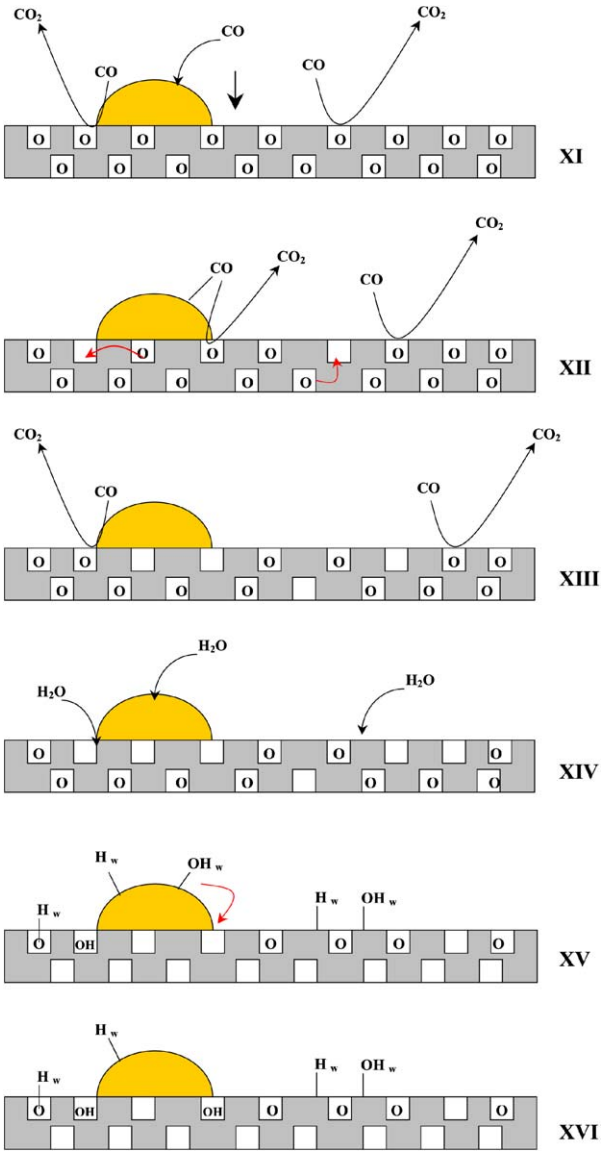

Fig. 16. Schematic model of WGS: XI–XIII—removal of oxygen atoms by CO, the lattice oxygen bulk diffusion; XIV–XVI—dissociative adsorption of H_2O and reoxidation of the reduced Fe_2O_3 by hydroxyl groups at the Au–support interface.

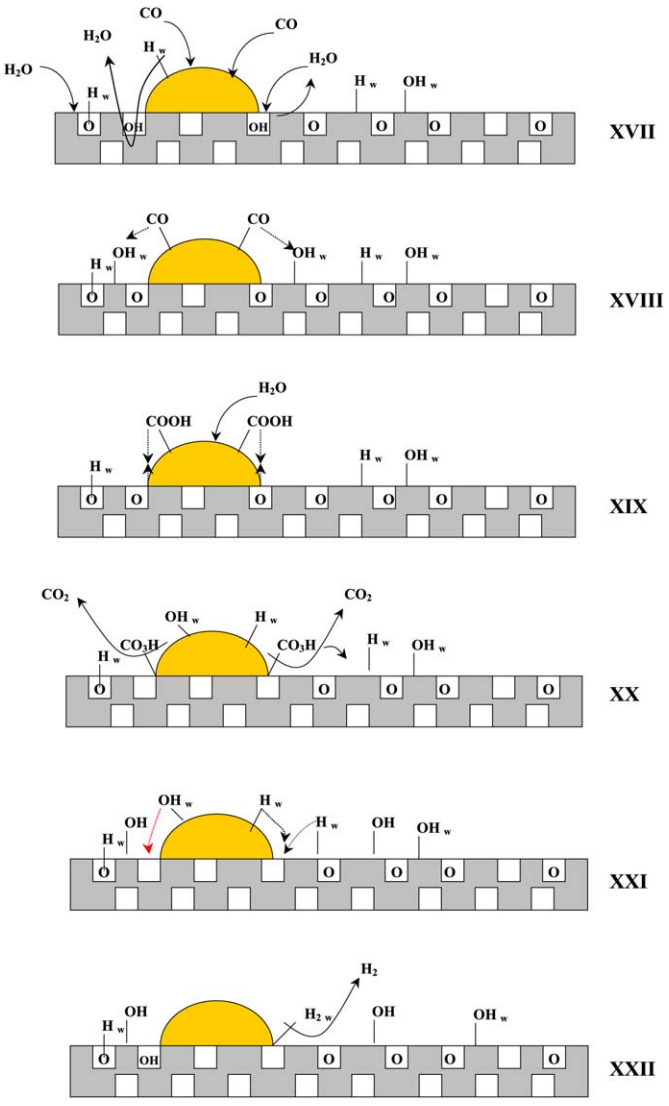

Fig. 17. Schematic model of WGS: XVII—reduction of support by hydrogen atom, linear adsorption of CO; XVIII, XIX—formation of carbonate species via reaction of adsorbed CO and present hydroxyl groups, spillover to Au–support interface; XX—formation of bicarbonates and their decomposition to CO and H_2O; XXI—reaction of hydrogen atoms on Au–support interface; XXII—release of H_2.

adsorptive mechanism considered for the Au/Fe_2O_3 catalysts by others [31,32,34,35] occurs via the formation of carbonates/bicarbonates as intermediates, not via the formation of formates. The formates in our work are only spectators and do not contribute to the production of CO_2. The formate mechanism for the WGS reaction has been postulated for Au/CeO_2 [23,27]. The formation of formate bands was observed on FTIR studies when Au/CeO_2 was exposed to CO and H_2O at 250 °C [23] and on DRIFTS studies in the temperature range of 200–350 °C [27]. Formates, formed by reaction with geminal OH groups, were assigned to be intermediates in the WGS mechanism over reduced CeO_2-supported Au catalyst [27].

According our observations at low temperatures, CO_2 formation proceeds via the adsorptive mechanism. The reducibility of Fe_2O_3 is minimal at such low temperatures (Fig. 3); the regenerative mechanism involving oxidation–reduction cycles plays a barely substantial role.

At high temperatures (i.e., 200 °C), at which Au catalysts have high catalytic activity for the WGS reaction and at which the WGS reaction is generally operated; the regeneration mechanism appears to make a substantial contribution to CO_2 and H_2O production. The Fe_2O_3 is easily reduced for Au/Fe_2O_3, and it alters a role of the support at in the WGS mechanism running at higher temperatures. Elevated temperatures are needed for the WGS reaction, and the fact that the catalyst is significantly reduced under steady-state conditions makes the formation and decomposition of (bi)carbonates less likely to play an essential role in the steady-state WGS reaction. A priori, the multistep formation and decomposition of carbonates is expected to be much slower than the direct removal of reactive

oxygen from Fe(III)-O followed by the reoxidation of these sites and the formation of H_2.

5. Conclusion

As-received Au/Fe_2O_3 contains carbonate-like species and hydroxyl groups, some of which are stable up to HTT at 400 °C. The remaining carbonates and hydroxyl groups are nevertheless reactive once the catalyst is exposed to CO at 25 °C.

Based on the DRIFTS spectra and *operando* transient experiments, we can deduce that the adsorptive mechanism of the WGS reaction consisting of the CO adsorption on Au particles, the formation of carbonates and bicarbonates at the Au–Fe_2O_3 interface, and their decomposition to CO_2 appears to prevail at room temperature. Formates play no role in this mechanism. At 200 °C (i.e., experimental conditions suitable for achieving a high activity of Au catalysts in the WGS reaction), the regenerative mechanism is dominant. Under these conditions, the catalyst support Fe_2O_3 is easily reducible in the presence of Au. The *operando* transient experiments also revealed that Au particles are essential for H_2 production and the reoxidation step involving H_2O as the reactant.

Acknowledgments

Funding was provided by the EU Training Network "Catalysis by Gold" (Auricat) (http://www.cf.ac.uk/chemy/staff/willock/Welcome.html). The authors thank Dr. B. Solsona, Cardiff University, for providing the Fe_2O_3 and Bart van der Linden for assisting with the DRIFTS and MS equipment and discussing the DRIFTS data.

References

[1] G.C. Bond, D.T. Thompson, Gold Bull. 33 (2000) 41.
[2] G.C. Bond, Catal. Today 72 (2002) 5.
[3] D. Cameron, R. Holliday, D. Thompson, J. Power Sources 118 (2003) 298.
[4] M. Haruta, T. Kobayshi, H. Sano, N. Yamada, Chem. Lett. (1987) 405.
[5] M. Haruta, N. Yamada, T. Kobayashi, S. Iijima, J. Catal. 115 (1989) 301.
[6] G.C. Bond, D.T. Thompson, Catal. Rev. Sci. Eng. 41 (1999) 319.
[7] M. Haruta, M. Daté, Appl. Catal. A 222 (2001) 427.
[8] G.J. Hutchings, Catal. Today 72 (2002) 11.
[9] M. Haruta, Catal. Today 36 (1997) 153.
[10] C.W. Corti, R.J. Holliday, D.T. Thompson, Appl. Catal. A 291 (2005) 253.
[11] R.M. Finch, N.A. Hodge, G.J. Hutchings, A. Meagher, Q.A. Pankhurst, M.R.H. Siddiqui, F.E. Wagner, R. Whyman, Phys. Chem. Chem. Phys. 1 (1999) 485.
[12] M.M. Schubert, M.J. Kahlich, H.A. Gasteiger, R.J. Behm, J. Power Sources 84 (1999) 175.
[13] N.M. Gupta, A.K. Tripathi, Gold Bull. 34 (4) (2001) 120.
[14] R.J.H. Grisel, B.E. Nieuwenhuys, J. Catal. 199 (2001) 48.
[15] M.M. Schubert, S. Hackenberg, A.C. van Veen, M. Muhler, V. Plzak, R.J. Behm, J. Catal. 197 (2001) 113.
[16] N.A. Hodge, C.J. Kiely, R. Whyman, M.R.H. Siddiqui, G.J. Hutchings, Q.A. Pankhurst, F.E. Wagner, R.R. Rajaram, S.E. Golunski, Catal. Today 72 (2002) 133.
[17] M. Manzoli, A. Chiorino, F. Boccuzzi, Appl. Catal. B 52 (2004) 259.
[18] S.T. Daniells, A.R. Overweg, M. Makkee, J.A. Moulijn, J. Catal. 229 (2005) 586.
[19] F. Moreau, G.C. Bond, A.O. Taylor, J. Catal. 231 (2005) 105.
[20] W. Deng, J. De Jesus, H. Saltsburg, M. Flytzani-Stephanopoulos, Appl. Catal. A 291 (2005) 126.
[21] D. Andreeva, V. Idakiev, T. Tabakova, L. Ilieva, P. Falaras, A. Bourlinos, A. Travlos, Catal. Today 72 (2002) 51.
[22] Q. Fu, H. Saltsburg, M. Flytzani-Stephanopoulos, Science 301 (2003) 935.
[23] T. Tabakova, F. Boccuzzi, M. Manzoli, D. Andreeva, Appl. Catal. A 252 (2003) 385.
[24] T. Tabakova, F. Boccuzzi, M. Manzoli, J.W. Sobczak, V. Idakiev, D. Andreeva, Appl. Catal. B 49 (2004) 73.
[25] G. Jacobs, P.M. Patterson, L. Williams, D. Sparks, B.H. Davis, Catal. Lett. 96 (2004) 97.
[26] Q. Fu, W. Deng, H. Saltsburg, M. Flytzani-Stephanopoulos, Appl. Catal. B 56 (2005) 57.
[27] G. Jacobs, E. Chenu, P.M. Patterson, L. Williams, D. Sparks, G. Thomas, B.H. Davis, Appl. Catal. A 258 (2004) 203.
[28] L. Luengnaruemitchai, S. Osuwan, E. Gulari, Catal. Commun. 4 (2003) 215.
[29] H. Sakurai, T. Akita, S. Tsubota, M. Kiuchi, M. Haruta, Appl. Catal. A 291 (2005) 179.
[30] H. Sakurai, A. Ueda, T. Kobayashi, M. Haruta, J. Chem. Soc. Chem. Commun. (1997) 271.
[31] F. Boccuzzi, A. Chiorino, M. Manzoli, D. Andreeva, T. Tabakova, J. Catal. 188 (1999) 176.
[32] D. Andreeva, Gold Bull. 35 (3) (2002) 82.
[33] T. Tabakova, V. Idakiev, D. Andreeva, I. Mitov, Appl. Catal. A 202 (2000) 91.
[34] D. Andreeva, V. Idakiev, T. Tabakova, A. Andreev, R. Giovanoli, Appl. Catal. A 134 (1996) 275.
[35] L.I. Illieva, D.H. Andreeva, A.A. Andreev, Termochim. Acta 292 (1997) 169.
[36] A. Vengopal, J. Aluha, M.S. Scurrell, Catal. Lett. 90 (2003) 1.
[37] A. Venugopal, M.S. Scurrell, Appl. Catal. A 258 (2004) 241.
[38] M.M. Mohamed, T.M. Salama, M. Ichikawa, J. Colloid Interface Sci. 224 (2000) 366.
[39] R.J. Davis, Science 301 (2003) 926.
[40] C. Rhodes, G.J. Hutchings, A.M. Ward, Catal. Today 23 (1995) 43.
[41] Seung-Jae Lee, A. Gavriilidis, J. Catal. 206 (2002) 305.
[42] N.M. Gupta, A.K. Tripathi, J. Catal. 187 (1999) 343.
[43] F. Boccuzzi, A. Chiorino, M. Manzoli, Ping Lu, T. Akita, S. Ichikawas, M. Haruta, J. Catal. 202 (2001) 256.
[44] M. Khoudiakov, M.C. Gupta, S. Deevi, Appl. Catal. A 291 (2005) 151.
[45] A.I. Kozlov, A.P. Kozlova, H. Liu, Y. Iwasawa, Appl. Catal. A 182 (1999) 9.
[46] G. Munteanu, L. Ilieva, D. Andreeva, Thermochim. Acta 291 (1997) 171.
[47] A. Milone, R. Ingoglia, A. Pistone, G. Neri, F. Frusteri, S. Galvagno, J. Catal. 222 (2004) 348.
[48] A. Davydov, Molecular Spectroscopy of Oxide Catalyst Surfaces, Wiley, Chichester, 2003.
[49] N.B. Colthup, L.H. Daly, S.E. Wiberley, Introduction to Infrared and Raman Spectroscopy, third ed., Academic Press, San Diego, 1990.
[50] C. Lemire, R. Meyer, Sh.K. Shaikhutdinov, H.-J. Freund, Surf. Sci. 552 (2004) 27.
[51] H. Sakurai, M. Haruta, Appl. Catal. A 127 (1995) 93.
[52] S.T. Daniells, M. Makkee, J.A. Moulijn, Catal. Lett. 100 (2005) 39.